Predicting Stomatal Closure and Turgor Loss in Woody Plants Using Predawn and Midday Water Potential[1][OPEN]

Thorsten Knipfer,[a,b,2] Nicolas Bambach,[a] M. Isabel Hernandez,[a] Megan K. Bartlett,[a] Gabriela Sinclair,[a] Fiona Duong,[a] Daniel A. Kluepfel,[c] and Andrew J. McElrone[a,c,3]

[a]Department of Viticulture and Enology, University of California, Davis, California 95616
[b]Faculty of Land and Food Systems, The University of British Columbia, Vancouver, British Columbia V6T 1Z4, Canada
[c]United States Department of Agriculture-Agricultural Research Service, Crops Pathology and Genetics Research Unit, Davis, California 95616

ORCID IDs: 0000-0001-5945-7273 (T.K.); 0000-0001-9889-5508 (M.I.H.)

Knowledge about physiological stress thresholds provides crucial information about plant performance and survival under drought. In this study, we report on the triphasic nature of the relationship between plant water potential (Ψ) at predawn and midday and describe a method that predicts Ψ at stomatal closure and turgor loss exclusively from this water potential curve (WP curve). The method is based on a piecewise linear regression model that was developed to predict the boundaries (termed Θ_1 and Θ_2) separating the three phases of the curve and corresponding slope values. The method was tested for three economically important woody species. For all species, midday Ψ was much more negative than predawn Ψ during phase I (mild drought), reductions in midday Ψ were minor while predawn Ψ continued to decline during phase II (moderate drought), and midday and predawn Ψ reached similar values during phase III (severe drought). Corresponding measurement of leaf gas exchange indicated that boundary Θ_1 between phases I and II coincided with Ψ at stomatal closure. Data from pressure-volume curves demonstrated that boundary Θ_2 between phases II and III predicted Ψ at leaf turgor loss. The WP curve method described here is an advanced application of the Scholander-type pressure chamber to categorize plant dehydration under drought into three distinct phases and to predict Ψ thresholds of stomatal closure and turgor loss.

Water stress by drought leads to plant mortality linked to carbon starvation and xylem hydraulic failure (Choat et al., 2018; McDowell et al., 2018). Plant survival under drought is dependent on a successful coordination of physiological responses across multiple organizational levels. This includes efficient stomatal regulation to limit excessive water loss to the atmosphere (Brodribb and Holbrook, 2003; Brodribb and McAdam, 2017), changes in root hydraulic and anatomical properties to minimize water loss to a drying soil and reduce the metabolic cost of soil exploration (Zhu et al., 2010; Barrios-Masias et al., 2015; Cuneo et al., 2016), and osmotic regulation and turgor maintenance on a cellular level to avoid negative effects on growth (Blum, 2017). The exact sequence of these physiological events needs to be elucidated across many species, but data indicate that drought-induced stomatal closure is well correlated with leaf turgor loss and the decline in leaf xylem hydraulic conductance (Brodribb and Holbrook, 2003). Scoffoni et al. (2018) showed that drought-induced changes in cell membrane permeability are linked to stomatal closure and that leaf xylem cavitation is negligible above the turgor loss point (Ψ_{TLP}). Recent reports suggest that stomatal closure is not triggered by xylem cavitation and primarily driven by a decline in root hydraulic conductance and changes within the root-to-soil hydraulic continuum (Carminati and Javaux, 2020; Rodriguez-Dominguez and Brodribb, 2020). For intact plants subjected to progressive drought stress, in vivo studies indicate that stomatal closure and root cortical cell

[1]This work was supported by the U.S. Department of Agriculture (grant no. 2032–22000–016–00D) and the American Vineyard Foundation (grant no. 2019–2284).

[2]Author for contact: tmknipfer@ucdavis.edu.
[3]Senior author.
The author responsible for distribution of materials integral to the findings presented in this article in accordance with the policy described in the Instructions for Authors (www.plantphysiol.org) is: Thorsten Knipfer (tmknipfer@ucdavis.edu).

T.K. designed and performed most of the experiments, analyzed the data, and wrote the article together with A.J.M.; N.B. developed the piecewise linear regression model, performed measurements on almond trees, and revised the article; M.I.H. helped with measurements of water potential, collected leaf pressure volume curves on walnuts, and revised the article; F.D. helped with measurement of water potential and leaf gas exchange on walnuts; M.K.B. acquired plant material, obtained funding for grapevine research, designed the grapevine experiment, and revised the article; G.S. performed measurements of water potential and leaf gas exchange on grapevines; D.A.K. obtained funding for walnut research, acquired the plant material, helped in experimental design, and revised the article; A.J.M. obtained funding, helped in experimental design, and wrote the article together with T.K.
[OPEN]Articles can be viewed without a subscription.
www.plantphysiol.org/cgi/doi/10.1104/pp.20.00500

damage precede xylem cavitation in the stem, which precedes the discharge of stored water from xylem fibers surrounding vessels (Cuneo et al., 2016; Knipfer et al., 2019).

Drought-induced stomatal closure plays an important role in minimizing excessive negative pressure in xylem sap (P_x), which contributes to increased drought resistance by reducing the risk of xylem cavitation (Martin-StPaul et al., 2017). Although a matter of debate, the isohydry/anisohydry concept provides a framework to describe the efficiency of a plant to control P_x and in turn plant water potential (Ψ) through stomatal opening/closing under drought (Tardieu and Simonneau, 1998; Martínez-Vilalta et al., 2014; Martínez-Vilalta and Garcia-Forner, 2017; Ratzmann et al., 2019). As suggested by Meinzer et al. (2016), maintenance of plant Ψ at midday (Ψ_{md}) while Ψ at predawn (Ψ_{pd}) declines is indicative for an isohydric behavior, while a decline in Ψ_{md} together with Ψ_{pd} points to an anisohydric behavior due to inefficient and/or uncoordinated stomatal closure. However, it remains elusive if Ψ thresholds corresponding to stomatal closure and leaf turgor (P) loss can be predicted directly from measurements of plant Ψ, but if so, this would certainly allow for a more time-effective and less labor-intensive assessment of both physiological responses.

The cohesion-tension theory predicts that transpirational pull drives the movement of xylem sap from roots to leaves (Dixon and Joly, 1895). The pressure chamber technique allows measuring plant Ψ in a relatively simple way and provides a good estimate of P_x when leaf apoplast is in equilibrium with symplast prior to leaf pressurization (Scholander et al., 1965; Turner, 1981). Commonly, the difference between measured plant Ψ and actual P_x is small, since the osmotic potential of the xylem sap is less than 0.1 MPa and the matric potential of the apoplast is close to Ψ of the symplast (Turner, 1981). For walnut (*Juglans* spp.) trees, Cochard et al. (2001) confirmed that the pressure chamber technique accurately predicts the existence of large negative P_x. Since plants function within a hydraulic continuum between soil and atmosphere, plant Ψ and P_x are dependent on the rate of water loss by transpiration and water uptake by roots. Because evaporative demand and light intensity change diurnally and impact transpiration via stomatal regulation, plant Ψ is most negative at midday (i.e. maximum transpiration) and least negative at predawn (i.e. negligible transpiration), especially under well-watered conditions (Klepper, 1968). Plant Ψ_{pd} provides an indicator for soil Ψ when nighttime transpiration is minimal and plants can reach an equilibrium with the wettest portion of the soil (Turner, 1981; Donovan et al., 2001). On the other hand, progressive drought stress results in a general decline in plant Ψ due to limitations in root water uptake and the fact that evaporative demand is not matched by water supply from the soil. In summary, plant Ψ measurements can provide an integrative measure of plant physiological responses to water stress by drought, but the relationship of Ψ_{pd} and Ψ_{md} under these conditions is surprisingly understudied.

About 40 years ago, Turner and Long (1980) showed that the relationship of Ψ measured on a covered (nontranspiring) and uncovered (transpiring) leaf is nonlinear for plants subjected to progressive drought stress, which highlighted the variable effect of transpiration on measurements of leaf Ψ. Martínez-Vilalta et al. (2014) presented a first theoretical framework regarding the relationship of leaf Ψ measured at midday and predawn, and the authors interpreted the slope of the relationship as the relative sensitivity of transpiration rate to increasing water stress by drought and the intercept as the maximum transpiration rate per unit of hydraulic transport capacity. Similarly, Meinzer et al. (2016) considered the impact of stomatal regulation on plant Ψ and found that the relationship of Ψ_{pd} and Ψ_{md} (i.e. measured following leaf covering and equilibration) is correlated with a species' Ψ_{TLP} and degree of isohydricity/anisohydricity (i.e. slope of curve and hydroscape). In contrast, Williams and Araujo (2002) reported that the relationship of Ψ_{pd} and Ψ_{md} is linear, but this finding may not hold true under more severe drought and stomatal closure. We revisited these findings for walnut, grapevine (*Vitis* spp.), and almond (*Prunus dulcis*) and performed an in-depth analysis of the water potential curve (WP curve) between Ψ_{pd} and Ψ_{md}. Measurements of Ψ_{pd} and Ψ_{md} were complemented with measurements of leaf gas exchange (stomatal conductance [g_s] and CO_2 assimilation rate [A]) for walnut and grapevine. In addition, for walnut, leaf sap osmotic pressure (π) and pressure-volume curves were collected to obtain an estimate of leaf P and Ψ at P loss. To test if characteristics of the WP curve are dependent on the type of drought experiment (Gilbert and Medina, 2016), walnut trees were subjected to a slow (weeks) and fast (days) drydown (not irrigated). For analysis of the WP curve, a mathematical approach was developed to determine the phases of plant dehydration and to calculate boundaries Θ_1 and Θ_2 separating phases I and II and phases II and III, respectively. Together, this allowed us to test the hypothesis that calculated Θ values from the WP curve predict Ψ at stomatal closure and leaf P loss. To avoid confusion, we will not use the existing terminology of Ψ_{leaf} and Ψ_{stem}, since in both cases Ψ is measured on an excised leaf that is either bagged for a relatively short (less than 10 s and nonequilibrated) or long (more than 15 min and equilibrated) time period, respectively.

RESULTS

Walnut

The relationship between Ψ_{pd} and Ψ_{md} exhibited a nonlinear behavior for walnut trees subjected to the slow drydown (Fig. 1A) and the fast drydown (Fig. 1C). Reductions in Ψ_{pd} and Ψ_{md} during the slow and fast

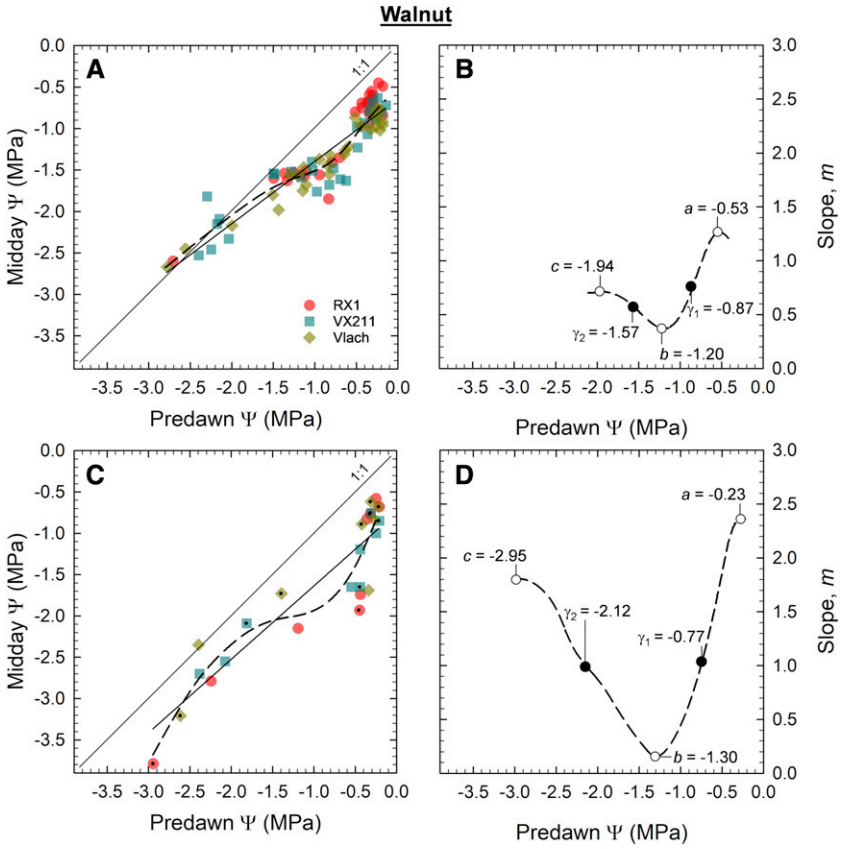

Figure 1. Relationship between plant Ψ_{pd} and Ψ_{md} for walnut trees ('Cisco'). Trees were subjected to a slow drydown (A and B; controlled irrigation over weeks) or a fast drydown (C and D; no irrigation over days). Data are summarized for trees grafted on rootstocks RX1, VX211, and Vlach. A and C, The dashed line is a smoothed line (smoothing factor = 60) that best followed the pattern of data points. The solid line is a linear regression fitted across data points (in A, R^2 = 0.87, m = 0.75, $P < 0.0001$; in B, R^2 = 0.85, m = 0.89, $P < 0.0001$). For C, during the fast drydown, the same symbols indicate data collected for the same tree. B and D, Relationship of Ψ_{pd} and slope values derived for the smoothed lines in A and C. Parameters a and c are the maximum slope values, parameter b is the minimum slope value, and γ_1 and γ_2 are the calculated transition points.

drydown were associated with a decline in soil moisture from around 75% to 45% (w/w) and 80% to 50% (w/w), respectively (Supplemental Fig. S1). In general, the relationship between Ψ_{pd} and Ψ_{md} can be described as follows: early during drought stress, Ψ_{md} was much more negative than Ψ_{pd}; this was followed by minor reductions in Ψ_{md} while Ψ_{pd} continued to decline under moderate drought; Ψ_{md} and Ψ_{pd} were most similar under severe drought stress (Fig. 1, A and C).

Based on the smoothed line fit included in Figure 1, A and C, transition points (γ) along the WP curve were calculated from $d\Psi_{md}/d\Psi_{pd}$ slope values (Fig. 1, B and D). Transition points of γ_1 and γ_2 were necessary to parameterize the piecewise linear regression (PLR) model. Subsequently, statistical estimates for boundary Θ_1 between phases I and II and boundary Θ_2 between phases II and III were obtained. The model predicted a boundary Θ_1 for the slow and fast drydown of -0.8 and -0.5 MPa, respectively (Fig. 2; Table 1). Comparing both drydown experiments, Θ_1 was less negative (by around 0.3 MPa) during the fast drydown. Boundary Θ_2 was at -1.3 (slow) and -2.2 MPa (fast), and Θ_2 was more negative (by around 0.9 MPa) during the fast drydown (Fig. 2). Representative images taken during the slow drydown showed that leaves appeared dark green and turgid for trees in phase I, leaves lost turgidity and appeared droopy at boundary Θ_2 in phase II, and leaves decolored to light green and started to desiccate and senesce at the bottom of the canopy in phase III (Supplemental Fig. S2).

The boundary Θ_1 between phases I and II corresponded to the Ψ threshold at which leaf gas exchange was substantially reduced in walnut trees (Fig. 3). The different values of Θ_1 as determined during the slow and fast drydown with the PLR model reflected the shift in Ψ threshold at which g_s and A reached a minimum. For the slow drydown, g_s and A of a mature leaf were reduced by 89% and 86%, respectively, when reaching boundary Θ_1 (Fig. 3, A and B). These reductions were similar for the fast drydown (Fig. 3, C and D).

The boundary Θ_2 between phases II and III corresponded to the Ψ threshold that marked the end of the leaf P maintenance phase and was indicative of the Ψ_{TLP} ($= -1.4 \pm 0.14$ MPa; Fig. 4; Supplemental Table S1). For the slow drydown, leaf P initially declined by around 60% during phase I, P was maintained during phase II, and subsequently P declined again during phase III (Fig. 4A). These drought-induced changes in P were associated with an increase in leaf sap π (Fig. 4B). For the fast drydown, P declined predominantly during phase I (Fig. 4C), similar to the slow drydown. However, given the drydown speed, we were not able to collect enough data points of P and π to conclusively report on the pattern of data points in phases II and III (Fig. 4, C and D).

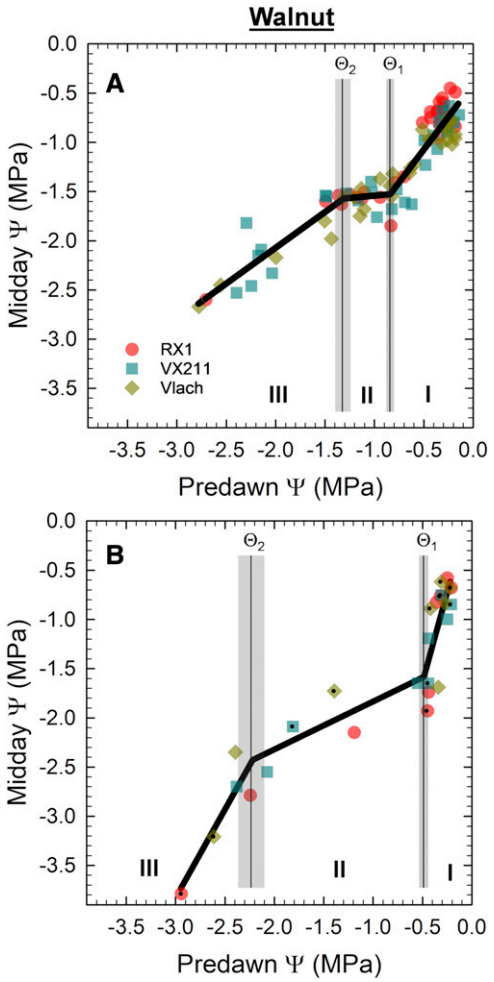

Figure 2. PLR model describing the triphasic relationship between Ψ_{pd} and Ψ_{md} for walnut trees. Models are shown as a thick solid lines. Data are shown for trees subjected to a slow drydown (A; corresponding to Fig. 1, A and B) or a fast drydown (B; corresponding to Fig. 1, C and D). For B, during the fast drydown, the same symbols indicate data collected for the same tree. Roman numerals I to III designate the three phases of the WP curve. Vertically solid lines are the boundaries between phases I and II (Θ_1) and phases II and III (Θ_2), and corresponding SE values are indicated in gray color. Model output parameters are summarized in Table 1.

Grapevine

The relationship between Ψ_{pd} and Ψ_{md} was nonlinear (from 0 to −2.5 MPa) for grapevine plants subjected to a slow drydown (Fig. 5). Following the initiation of water stress by drought, Ψ_{md} was more negative than Ψ_{pd} (see deviation from the 1:1 line). Subsequently, reductions in Ψ_{md} were minor while Ψ_{pd} continued to decline under moderate drought; values of Ψ_{md} and Ψ_{pd} were most comparable under severe drought (Fig. 5A). Following the smoothed line fit, the transition points along the WP curve were located at γ_1 of −0.58 MPa and γ_2 of −1.57 MPa (Fig. 5B). The PLR model predicted for grapevine that boundary Θ_1 between phases I and II was at −0.68 MPa and boundary Θ_2 between phases II and III was at −1.33 MPa (Fig. 6; Table 1).

Leaf gas exchange was measured for grapevine (Fig. 7). This showed that boundary Θ_1 between phases I and II matched the Ψ threshold at which leaf gas exchange was substantially reduced (Fig. 7). Following an initial increase of g_s (Fig. 7A) and A (Fig. 7B), that reached a maximum at Ψ_{pd} of around −0.4 MPa, g_s and A declined by 93% and 67%, respectively, thereafter reaching values of close to zero at boundary Θ_1.

Almond

Similar to data collected for potted walnut (Fig. 2) and grapevine (Fig. 6) plants, data collected for almond trees showed that the relationship of Ψ_{pd} and Ψ_{md} exhibited a triphasic curve shape (Fig. 8). The calculated boundary values using our PLR model were $\Theta_1 = -1.37$ MPa and $\Theta_2 = -1.94$ MPa (Fig. 9; Table 1). See Supplemental Table S2 for statistical comparison of all output parameters obtained with the PLR model (Table 1).

DISCUSSION

In this study, we describe a method that allows predicting stress thresholds associated with drought-induced stomatal closure and turgor loss exclusively from measurements of plant Ψ using a Scholander-type pressure chamber. For woody species (walnut, grapevine, and almond), we found that the WP curve between plant Ψ at midday and predawn exhibits a unique triphasic curve shape. To quantify the underlying curve parameters, we developed a PLR model for statistical analysis of the WP curve. For walnut and grapevine, modeling data together with leaf gas-exchange data indicated that boundary Θ_1 between phases I and II marked the Ψ threshold at which g_s was reduced by around 90%. For almond, leaf gas exchange was reduced by approximately 70% at Ψ_{pd} of −1.4 MPa (Marsal et al., 1997), and this suggests that our calculated boundary Θ_1 at −1.37 MPa for cv Nonpareil most likely predicts stomatal closure as well. Our data of leaf π and Ψ_{TLP} from pressure-volume curves indicated that the boundary Θ_2 between phases II and III marked the end of the leaf P maintenance phase and Ψ at P loss for walnut. For grapevine and almond, literature data of Ψ_{TLP} (−1.4 MPa for grapevine 'Chardonnay' [Alsina et al., 2007] and −2.1 MPa for almond 'Garrigues' [Torrecillas et al., 1996]) closely matched our calculated Θ_2. The robustness of our WP curve method was tested for walnut by analyzing two types of drydown experiments (slow over weeks versus fast over days and no irrigation). This showed that the WP curve method was successful in identifying the shift in Ψ at stomatal closure depending on the type of drought experiment. Moreover, preliminary data collected for commercially

Table 1. *Summary of output parameters from the PLR model as used for analysis of the relationship between Ψ_{pd} and Ψ_{md} for woody species (walnut 'Cisco', grapevine 'Chardonnay', and almond 'Nonpareil')*

Parameters are as follows: N = number of observations, Θ_1 = boundary between phases I and II, Θ_2 = boundary between phases II and III, β_1 = slope phase I, β_2 = slope phase II, β_3 = slope phase III, α = intercept, and R^2 = coefficient of determination. n/a, Not applicable.

Parameter	Walnut						Grapevine			Almond		
	Figure 2A			Figure 2B			Figure 6			Figure 9		
	Value	SE	*P*	Value	SE	*P*	Value	SE	*P*	Value	SE	*P*
N	92	n/a	n/a	24	n/a	n/a	80	n/a	n/a	336	n/a	n/a
Θ_1 (MPa)	−0.84	0.08	<0.01	−0.49	0.10	<0.01	−0.68	0.14	<0.01	−1.37	0.11	<0.01
Θ_2 (MPa)	−1.31	0.16	<0.01	−2.22	0.26	<0.01	−1.33	0.44	<0.01	−1.94	0.09	<0.01
β_1	1.33	0.23	<0.01	3.64	0.57	<0.01	1.23	0.63	0.05	0.98	0.19	<0.01
β_2	0.09	0.20	<0.01	0.49	0.63	0.05	−0.03	1.02	0.17	0.23	0.20	<0.01
β_3	0.73	0.07	<0.01	1.80	0.95	<0.01	1.39	0.86	0.11	1.05	0.08	<0.01
α (MPa)	−0.62	0.08	<0.01	0.32	0.28	<0.01	0.60	0.24	<0.01	0.14	0.03	<0.01
R^2	0.91	n/a	n/a	0.90	n/a	n/a	0.62	n/a	n/a	0.95	n/a	n/a

available walnut rootstocks RX1 (*Juglans microcarpa* × *Juglans regia*) and VX211 (*Juglans hindsii* × *J. regia*) indicated that WP curves are genotype specific (Supplemental Fig. S3). In summary, the WP curve method provides for a new approach to evaluate plant drought responses (stomatal closure and turgor loss) in a cost-effective and relatively simple way that only requires access to a Scholander-type pressure chamber.

Drought-Induced Stomatal Closure

In the past, Turner and Long (1980) reported on the nonlinear behavior of the relationship of Ψ measured simultaneously on a covered leaf prior to excision and an uncovered leaf. Their data show a triphasic curve shape with values approaching 1:1 due to stomatal closure when plants experience severe drought. Similarly, our data demonstrate that the relationship of Ψ_{pd} and Ψ_{md} is nonlinear and triphasic. Our leaf gas-exchange measurements indicated that g_s started to reach a minimum at the transition point between phases I and II (i.e. boundary Θ_1) of the WP curve, which confirmed that stomatal closure was the main driver that caused the initial change in shape of the WP curve. We speculate that the shape of the curve between g_s and Ψ_{pd} until reaching boundary Θ_1 is dependent on how

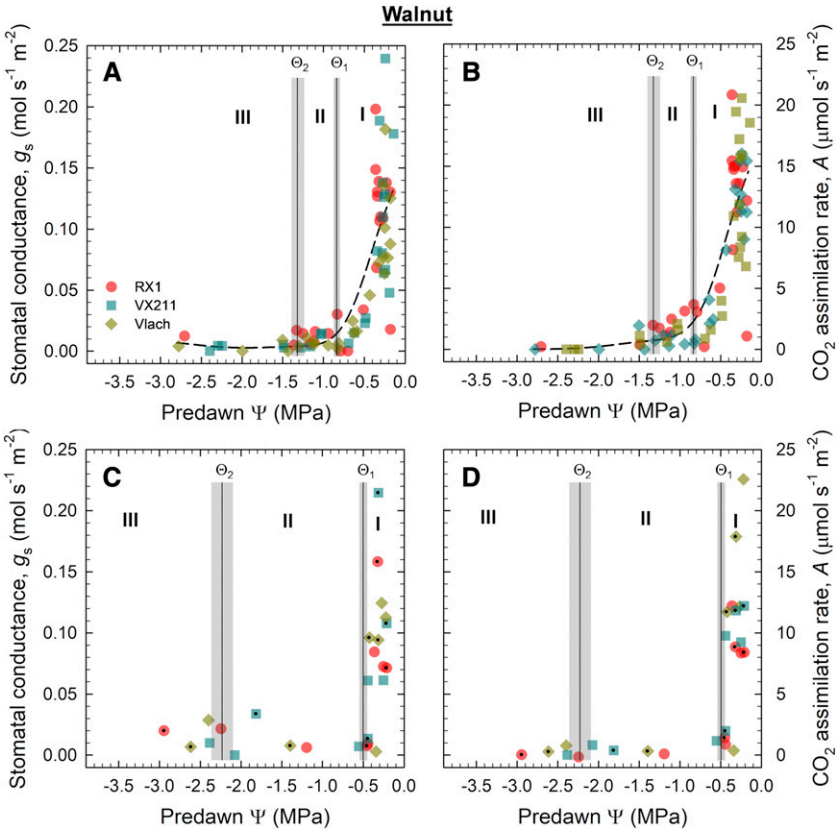

Figure 3. Relationship between Ψ_{pd} and leaf gas exchange (g_s [A and C] or A [B and D]) for walnut trees. Trees were subjected to a slow drydown (A and B) or a fast drydown (C and D). For C and D, during the fast drydown, the same symbols indicate data collected for the same tree. Roman numerals I to III designate the three phases of the WP curve (corresponding to Fig. 2). Vertically solid lines are the boundaries between phases I and II (Θ_1) and phases II and III (Θ_2), and corresponding SE values are indicated in gray color. A and B, The dashed line is a smoothed line (smoothing factor = 60) that best described the pattern of data points. C and D, Due to the limited amount of data points collected during the fast drydown for phases II and III, a fitted line is not included.

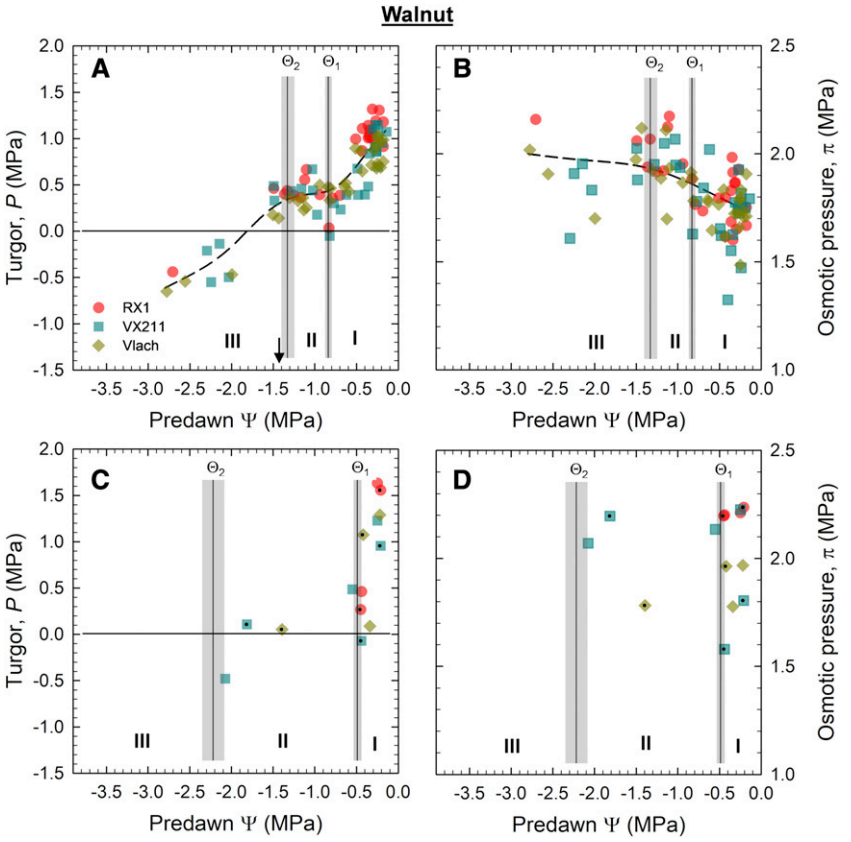

Figure 4. Relationship between Ψ_{pd} and leaf cell pressure (P [A and C] or sap π [B and D]) for walnut trees. Trees were subjected to a slow drydown (A and B) or a fast drydown (C and D). For C and D, during the fast drydown, the same symbols indicate data collected for the same tree. Roman numerals I to III designate the three phases of the WP curve (corresponding to Fig. 2). Vertically solid lines are the boundaries between phases I and II (Θ_1) and phases II and III (Θ_2), and corresponding SE values are indicated in gray color. A and B, The dashed line is a smoothed line (smoothing factors = 60 in A and 75 in B) that best described the pattern of data points. The arrow in A indicates the average leaf Ψ_{TLP} of -1.4 ± 0.14 MPa as measured from pressure-volume curves (Supplemental Table S1). C and D, Due to the limited amount of data points collected during the fast drydown for phases II and III, a fitted line is not included.

well drought-induced closure between individual stomates of a leaf is coordinated. For example, a distinctive drop-off in measured g_s should only be observed at boundary Θ_1 when all stomates transition instantaneously from an open to a closed state (Gollan et al., 1985). Following this logic, we hypothesize that the shape of the WP curve during phase I is predominantly affected by the ability of a plant to efficiently coordinate stomatal closure under increasing water stress by drought.

Stomatal closure/opening can be triggered by several factors, including light intensity, vapor pressure deficit (VPD), abscisic acid (ABA) concentration, and/or hydrostatic pressure (Farquhar and Sharkey, 1982; Franks, 2013; Tombesi et al., 2015). We did not measure ABA concentrations, but the role of ABA in stomatal closure can be summarized as follows. A root tip that is exposed to dry soil conditions commonly synthesizes additional amounts of ABA, which ultimately arrives in leaves depending on the transport efficiency of the transpiration stream (Zhang et al., 1987). Gollan et al. (1986) showed that when leaves are kept turgid by pressurizing roots while the soil is drying, stomates still closed, which was interpreted as further evidence for

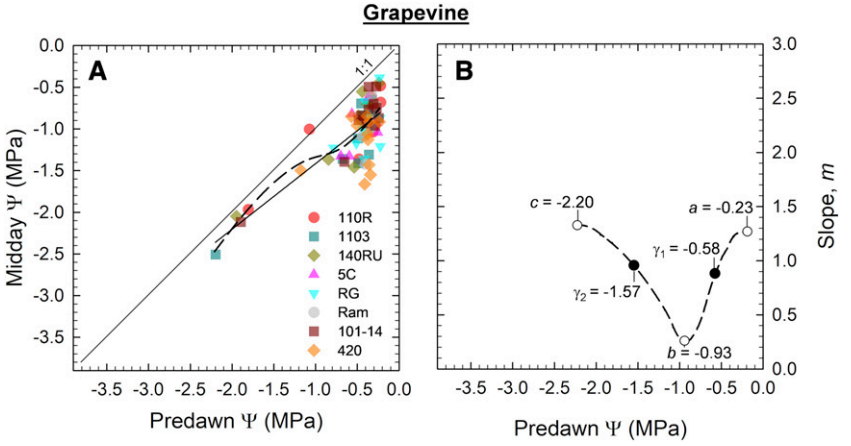

Figure 5. Relationship between Ψ_{pd} and Ψ_{md} for grapevine ('Chardonnay'). Data are summarized for cv Chardonnay grafted on rootstocks 110R, 1103, 140RU, 5C, RG, Ramsey, 101-14, and 420. A, The dashed line is a smoothed line (smoothing factor = 60) that best followed the pattern of data points. The solid line is a linear regression fitted across data points ($R^2 = 0.59$, $m = 0.79$, $P < 0.0001$). B, Relationship of Ψ_{pd} and slope values derived for the smoothed line in A. Parameters a and c are the maximum slope values and parameter b is the minimum slope value, and γ_1 and γ_2 are the calculated transition points.

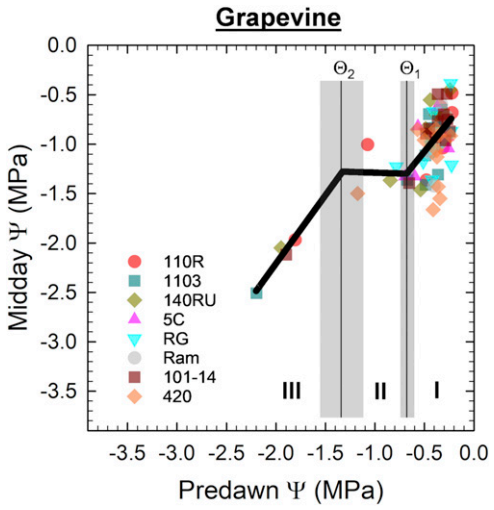

Figure 6. PLR model describing the triphasic relationship between Ψ_{pd} and Ψ_{md} for grapevine (corresponding to Fig. 5). The model is shown as a thick solid line. Roman numerals I to III designate the three phases of the WP curve. Vertically solid lines are the boundaries between phases I and II (Θ_1) and phases II and III (Θ_2), and corresponding SE values are indicated in gray color. Model output parameters are summarized in Table 1.

the importance of root-to-shoot signaling via ABA translocation. However, McAdam and Brodribb (2018) found that leaf mesophyll cells are the main location for ABA biosynthesis under drought stress, which deemphasizes the importance of ABA delivery from roots to leaves via the xylem to initiate stomatal closure. Drought-induced increases in root ABA concentrations may also trigger aquaporin-mediated changes in root hydraulic conductivity and/or result in modifications of root architecture (Aroca et al., 2012). Recent studies suggest that drought-induced changes in root and soil hydraulic properties drive stomatal closure (Carminati and Javaux, 2020; Rodriguez-Dominguez and Brodribb, 2020). Besides ABA, drought-induced stomatal closure can be mediated by a pressure-induced passive mechanism depending on P_x (Brodribb and McAdam, 2011; Franks, 2013). Tombesi et al. (2015) reported that g_s in grapevine subjected to drought stress is predominantly regulated by such a passive hydraulic signal. The authors came to this conclusion because leaf ABA increased only after complete stomatal closure, and it was hypothesized that this is of importance for long-term drought recovery to facilitate xylem embolism repair by forcing stomatal closure when the soil is rehydrated. In summary, and in the context of collecting WP curves for various woody plants, we speculate that if leaf ABA accumulation is observed in phase I, this points to a predominant ABA-mediated mechanism driving stomatal closure, whereas if leaf ABA accumulation is observed in phase II, this points to a predominant pressure-driven (passive) mechanism driving stomatal closure.

Atmospheric evaporative demand affects the rate of transpiration (see introduction; Klepper, 1968). Gollan et al. (1985) performed an extensive study on the relationship of VPD, Ψ determined on leaves with in situ psychrometers, and soil water content on leaf gas exchange. The authors showed that the relationship of Ψ and leaf gas exchange is dependent on VPD. During increasing drought, their data point to a sharp drop-off in g_s at high VPD (25 Pa kPa^{-1}), whereas the reduction in g_s was gradual until reaching a minimum (as observed in this study) at low VPD (10 Pa kPa^{-1}). Due to natural fluctuations in VPD and its effect on transpiration, plant Ψ can vary between days and over the course of a day for the same soil water status. For this reason, Ψ_{md} (as measured on an equilibrated leaf using a pressure chamber [i.e. Ψ_{stem}]) is most meaningful as a water stress indicator over the growing season when compared with baseline values under well-irrigated conditions (Turner, 1990; Shackel et al., 1997). Based on our findings, we hypothesize that the effects of VPD on the shape of the WP curve are most pronounced during phase I prior to stomatal closure, and high versus low VPD conditions result in either a steeper (higher transpiration) or shallower (lower transpiration) slope β_1. On the other hand, and for a given plant species, we speculate that the effect of VPD on boundary Θ_1 is negligible if stomatal closure is

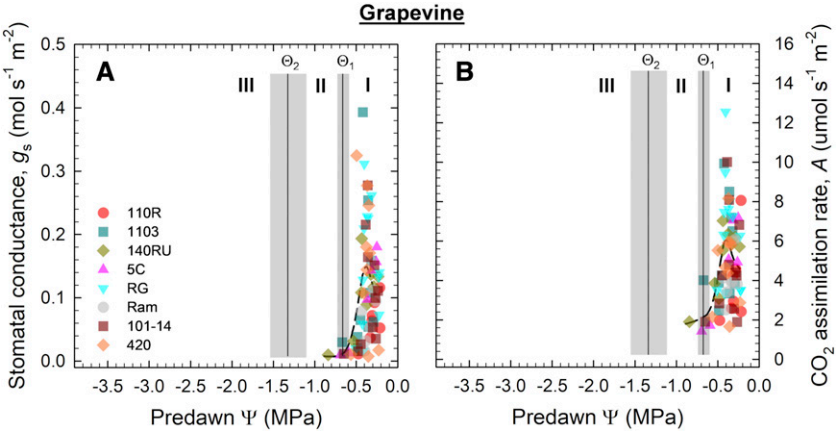

Figure 7. Relationship between Ψ_{pd} and leaf gas exchange (g_s [A] or A [B]) for grapevine (corresponding to Figs. 5 and 6). The dashed line is a smoothed line (smoothing factor = 60) that best described the pattern of data points. Since leaf gas exchange reached a minimum at Ψ_{pd} of around −0.7 MPa, additional data were not collected past this point. Roman numerals I to III designate the three phases of the WP curve (corresponding to Fig. 6). Vertically solid lines are the modeled boundaries between phases I and II (Θ_1) and phases II and III (Θ_2), and corresponding SE values are indicated in gray color.

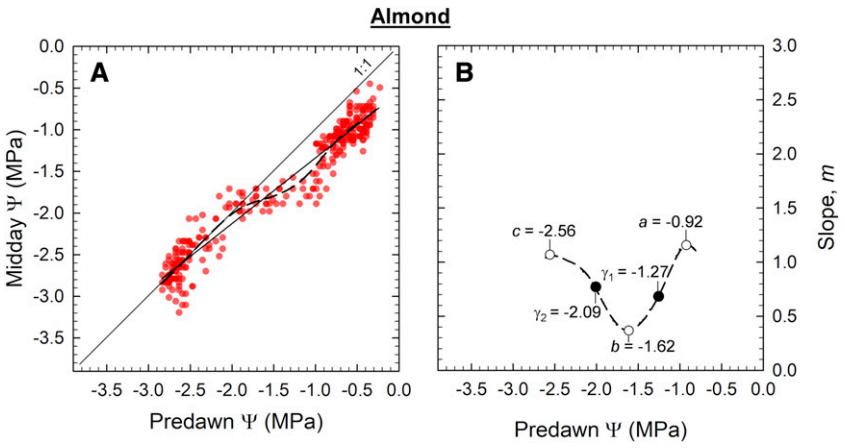

Figure 8. Relationship between Ψ_{pd} and Ψ_{md} for almond ('Nonpareil'). A, Data were obtained for trees grafted onto rootstock Nemaguard. The dashed line is a smoothed line (smoothing factor = 60) that best followed the pattern of data points. The solid line is a linear regression fitted across data points ($R^2 = 0.94$, $m = 0.79$, $P < 0.0001$). B, Relationship of Ψ_{pd} and slope values derived for the smoothed line in A. Parameters *a* and *c* are the maximum slope values, parameter *b* is the minimum slope value, and γ_1 and γ_2 are the calculated transition points.

predominantly driven by soil-to-root interactions (see previous paragraph).

Leaf Turgor Loss

Our data provide evidence that boundary Θ_2 separating phases II and III of the WP curve predicts Ψ_{TLP}. For walnut ('Cisco'), average Ψ_{TLP} determined from pressure-volume curves of −1.39 MPa (Supplemental Table S1) was only slightly more negative as compared with Θ_2 of −1.31 MPa (Table 1). For grapevine ('Chardonnay'), Alsina et al. (2007) reported an average Ψ_{TLP} of −1.36 MPa at veraison and prior to berry maturation, which was similar to our Θ_2 of −1.33 MPa (Table 1). For almond, Torrecillas et al. (1996) determined a Ψ_{TLP} of around −2.2 MPa (cv Garrigues) and −2.3 MPa (cv Ramilete) for well-watered trees as compared with our Θ_2 of −1.9 MPa (cv Nonpareil; Table 1). Together, these findings suggest that Ψ_{TLP} can be predicted from the triphasic WP curve using our PLR model for a variety of woody species.

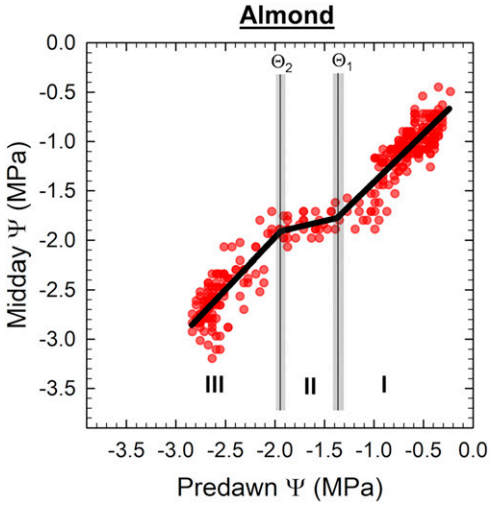

Figure 9. PLR model describing the triphasic relationship between Ψ_{pd} and Ψ_{md} for almond trees (corresponding to Fig. 8). The model is shown as a thick solid line. Roman numerals I to III designate the three phases of the WP curve. Vertically solid lines are the boundaries between phases I and II (Θ_1) and phases II and III (Θ_2), and corresponding SE values are indicated in gray color. Model output parameters are summarized in Table 1.

For walnut trees subjected to the slow drydown, we were able to collect sufficient data points to elucidate the pattern of drought-induced variations in *P* ($P = \Psi - \pi\sigma$). To calculate *P*, we assumed that $\pi \approx \pi_{symplast}$ and that the reflection coefficient for solutes (σ) was unity. If we consider that the remaining apoplastic sap in the centrifuged leaf tissue resulted in a dilution effect (Wardlaw, 2005), then our measured π underestimated true $\pi_{symplast}$. Hence, true *P* should be slightly lower than our calculated *P*, which would explain why our calculated *P* was 0.3 MPa and not 0 MPa at Θ_2 of −1.31 MPa (Fig. 4A). On the other hand, π_o at full hydration obtained from pressure-volume curves was 1.1 MPa (Supplemental Table S1) but π at Ψ_{pd} of 0 MPa was around 1.7 MPa (Fig. 4A), which points to a possible overestimation of $\pi_{symplast}$. The indirect approach used here provides a relatively easy way to obtain information on drought-induced *P* changes, but if experimentally feasible, *P* and $\pi_{symplast}$ are best determined directly using a combination of cell pressure probing and picoliter osmometry (Tomos and Leigh, 1999; Fricke and Peters, 2002; Knipfer et al., 2014).

Although controversial, it has been reported that negative *P* exists in plant cells according to indirect measurements from pressure-volume curves (Tyree, 1976; Rhizopoulou, 1997; Ding et al., 2014). Our *P* data obtained indirectly by $\Psi - \pi\sigma$ also point to the existence of negative *P*, which occurred in phase III following the Ψ_{TLP}. However, one factor that may explain the measurement of negative *P* when determined indirectly is σ, which provides a measure of solute permeability/leakage of the cell membrane (Staverman, 1951; Knipfer et al., 2014). Drought stress results in increased solute leakage and modulation of the physical state of the membrane (Blum and Ebercon, 1981; Premachandra and Shimada, 1987; Couchoud et al., 2019). If solute leakage plays a role during

drought stress, then P is best determined by $\Psi - \pi\sigma_i$ where i = level of water stress. Hence, if we imagine that solute leakage becomes more and more severe under increasing drought stress, σ would become smaller and smaller and the term $\sigma\pi$ goes toward zero, which in turn would result in a calculated P that may not reach negative values. Comparing the slow versus fast drydown, our data suggest that P reaches values closer to zero during the fast drydown at boundary Θ_1. This may be due to generally higher π values in mature leaves of these trees because of seasonal effects (i.e. this drydown was performed in September versus June/July) or less severe cell membrane damage and electrolyte leakage during phase I when the drydown is fast (i.e. this drydown was performed over a couple of days versus weeks). However, the biophysical properties of the cell membrane under various levels of drought stress and in response to the type of the drought experiment remain unknown, and only direct P measurements using a cell pressure probe would allow us to resolve these open questions (see previous paragraph).

Pressure-Volume Curve

The Scholander-type pressure chamber has been used successfully to generate pressure-volume curves for the determination of tissue properties such as Ψ_{TLP}, bulk modulus of elasticity, and π_o at full hydration (Tyree and Hammel, 1972; Ding et al., 2014). The advantage of the pressure-volume curve is that Ψ_{TLP} can be determined from a single leaf measurement. The disadvantage is that generating a pressure-volume curve can be time consuming (more than 10 h) depending on the speed of leaf dehydration and requires accessibility to an analytical digital balance to determine relative water content; one technical difficulty is finding the right time interval for progressive leaf dehydration and data collection.

WP Curve

The WP curve method allows predicting Ψ at stomatal closure and Ψ_{TLP} exclusively from measurements of Ψ_{pd} and Ψ_{md} using a Scholander-type pressure chamber. This can be especially useful under remote field conditions or during research operations with limited access to a leaf gas-exchange system, analytical balance, and laboratory space. Moreover, the WP curve method can provide for a time-integrative measurement of Ψ at stomatal closure and Ψ_{TLP} when collected over the growing season. In this case, it is recommended that plant Ψ be measured during the phenological time frame following leaf maturation and prior to senescence to ensure that leaf cells, xylem, and cuticle are fully developed. For establishing the WP curve, we advocate the following stepwise procedure for the measurement of plant Ψ (Fig. 10).

Step 1: covering of leaf to minimize transpiration. Identify a representative mature leaf in the canopy and cover the leaf with a plastic bag. Seal the plastic bag to allow for a humid environment that aids stomatal closure and minimizes transpiration (Turner and Long, 1980).

Step 2: equilibration of leaf apoplast and symplast. Wrap the sealed plastic bag with aluminum foil to exclude ambient light from the leaf surface. This will further aid stomatal closure. Wait for more than 30 min to allow for equilibration of leaf internal Ψ of apoplast (liquid to the outside of the cellular membrane including xylem liquid) and symplast (liquid to the inside of the cellular membrane). Including the equilibration will ultimately provide a measure of plant Ψ that closely reflects P_x (see introduction).

Step 3: excision of the leaf. Cut the leaf at the petiole (or petiolule) end using scissors or a razor blade.

Step 4: measurement of plant Ψ. Insert the covered leaf into the pressure chamber with the cut surface protruding through the seal of the chamber lid. Slowly raise the pressure in the chamber while monitoring the cut surface; use a magnifying glass and a light source if it is difficult to identify xylem vessels. Record the pressure when liquid starts to emerge from open xylem vessels and a meniscus forms on the cut surface.

One alternative procedure to save time is to skip the equilibration step and immediately proceed from step 1 to step 3 (Fig. 10). However, excluding the equilibration step 2 provides a less accurate estimate of P_x, since leaf internal Ψ gradients between apoplast and symplast are not minimized prior to leaf excision (Shackel et al., 1997). Another alternative procedure is to seal the excised leaf in a second plastic bag (i.e. to minimize leaf water loss as much as possible) and store the sample at around 4°C for up to 24 h prior to measurement of plant Ψ (Fig. 10); the assumption is that leaf internal Ψ is maintained constant during the storage period, but this should ideally be tested first on a subset of leaves through frequent measurements of Ψ_{pd} and Ψ_{md} during the storage period.

Our data show that, opposite to a fast drydown, a controlled and slow drydown (weeks) has the advantage of collecting a higher number of data points during all three phases of the WP curve because Ψ_{pd} can be determined for a wide range of soil moisture contents. When establishing the WP curve, Ψ_{pd} can be interpreted as a measurement of soil Ψ when nighttime water loss by transpiration is negligible for the plants analyzed. For plant species that exhibit relatively high rates of nighttime transpiration, the required equilibrium between Ψ_{pd} and soil Ψ cannot be reached (Donovan et al., 2001). Donovan et al. (2001) came to this conclusion by comparing measurements of soil Ψ and Ψ_{pd} as obtained from plants with completely bagged and nonbagged canopies during the night period. For walnut trees subjected to the slow drydown, nighttime canopy conductance was more than 100-fold smaller compared with daytime values (Supplemental Fig. S4, inset), and we can conclude that our measurements of

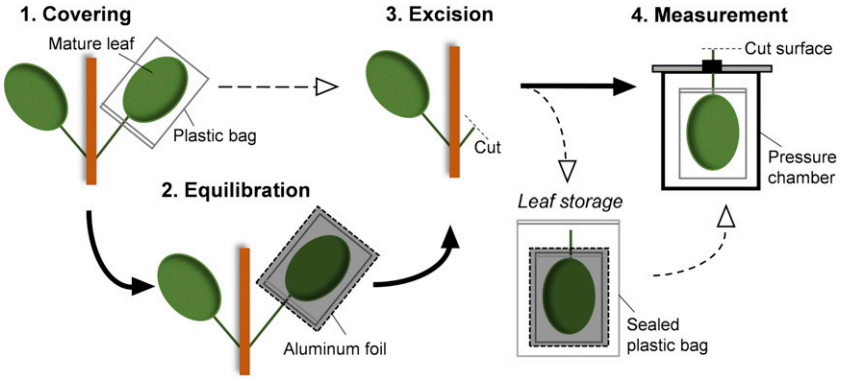

Figure 10. Scheme illustrating the stepwise procedure for the measurement of plant Ψ. Thick arrows indicate the sequence of steps that is recommended for generation of the WP curve. The equilibration step (greater than 30 min) ensures a final measurement of Ψ that best reflects the magnitude of negative xylem pressure. Dashed arrows indicate the sequence of alternative steps that may be followed to speed up the time between covering and excision (less than 10 s) and/or to allow for the transport of leaf samples and extend the time period between excision and measurement to several hours.

Ψ_{pd} closely reflected soil Ψ for this type of experiment. For every soil type, soil Ψ can be interpreted as the ability of a plant to extract water from the soil (Jones, 2007). However, the breakdown of the soil-to-root hydraulic continuum is suspected to be the trigger for stomatal closure (Carminati and Javaux, 2020). In turn, it can be speculated that boundary Θ_1 also provides an estimate when the hydraulic continuum between root and soil starts to break down under increasing water stress by drought independent of the soil type.

Type of Drought Experiment

Limited soil water availability is the factor that causes drought stress. Plant stress responses to drought depend on drought severity and a plant's ability to adapt to the stress over time (Gilbert and Medina, 2016). Therefore, the experimental procedure of how drought is induced over time (i.e. days versus weeks) can result in a more or less severe stress response for a given level of soil moisture. A slow drydown (weeks) would provide time for stress adaptations linked to plant anatomical changes, for example, root suberization to minimize water loss back to the soil and reductions in vessel diameters to secure long-distance transport capacity (Barrios-Masias et al., 2015; Knipfer et al., 2015, 2018, 2020). Here, we conducted slow and fast drydown experiments for walnut trees to test if the WP curve (1) remains triphasic and (2) predicts stomatal closure in both types of experiments. Our data show that the WP curve was triphasic in both drydown experiments, but the character of the WP curve differed between the slow and fast drydown and boundary values Θ_1 and Θ_2 were specific to the drydown experiment (Table 1). Boundary Θ_1 predicted the shift in the Ψ threshold of stomatal closure in both types of drydown experiment. We speculate that boundary Θ_1 was less negative during the fast drydown (i.e. earlier stomatal closure) because the time period for anatomical adaptations, which would aid in maintaining plant performance for the imposed level of stress, was too short. Data by Knipfer et al. (2020) show that walnut fine roots develop a multiseriate endodermis in response to a slow drydown, and data by Meyer et al. (2009) indicate that the development of a multiseriate exodermis in *Iris germanica* requires ~12 d. However, and especially for the purpose of using the WP curve method to select for genotypes with improved drought resistance, future work is required to exactly determine the effects of experimental time period, soil medium, irrigation frequency, and pot characteristics on the shape of the WP curve (Turner, 2019).

CONCLUSION

The WP curve method represents a methodological advancement of the Scholander-type pressure chamber to predict Ψ at stomatal closure and turgor loss. Based exclusively on measurements of plant Ψ at predawn and midday, the method presented here provides an alternative tool for the study of plant stress physiology in natural and agricultural ecosystems. According to published data for grapevine and under the assumption that plant Ψ reported by these authors (i.e. measured under laboratory low-light conditions) is most representative of Ψ_{pd} (Choat et al., 2010; Brodersen et al., 2013; Cuneo et al., 2016), the following can be concluded: (1) root cell damage is initiated at boundary Θ_1 at a Ψ threshold that corresponds to stomatal closure; (2) root hydraulic conductivity declines progressively during phases I and II and reaches a minimum at boundary Θ_2 at a Ψ threshold that corresponds to leaf turgor loss; and (3) vessel cavitation is initiated at boundary Θ_2 and cavitated vessels accumulate during phase III. This example demonstrates that our WP curve method can be used to categorize the sequence of physiological and anatomical events that occur under progressive drought stress into three distinct phases. Moreover, we propose that the WP curve method can assist in the determination of Ψ thresholds that mark the breakdown of the soil-to-root hydraulic continuum (Carminati and Javaux, 2020; Rodriguez-Dominguez and Brodribb, 2020) and xylem hydraulic failure by embolism (Cuneo et al., 2016; Knipfer et al., 2019) and facilitate the selection for woody perennial genotypes with improved drought resistance (Knipfer et al., 2020).

MATERIALS AND METHODS

PLR Model

Initial data inspection showed that a simple linear model did not appropriately describe the relationship of plant Ψ_{pd} and Ψ_{md} for three woody species, walnut (*Juglans* spp.), grapevine (*Vitis* spp.), and almond (*Prunus dulcis*). For this reason, the PLR model was developed for analysis of the WP curve:

$$\Psi_{md}(\Psi_{pd}) = \begin{cases} \alpha + \beta_3\Psi_{pd}\ , & \Psi_{pd} \le \Theta_2 \\ \alpha + \Theta_2(\beta_3 - \beta_2) + \beta_2\Psi_{pd}\ , & \Theta_1 \ge \Psi_{pd} > \Theta_2 \\ \alpha + \Theta_2(\beta_3 - \ \beta_2) + \Theta_1(\beta_2 - \beta_1) + \beta_1\Psi_{pd}\ , & \Psi_{pd} > \Theta_1 \end{cases}$$

The PLR model was used to calculate the boundaries between linear phases (Θ_1 = phase I to II and Θ_2 = phase II to III) and corresponding slope values (β_1 = phase I, β_2 = phase II, and β_3 = phase III; α = intercept).

To parameterize the PLR model, an estimate of the transition points between phases I and II (γ_1) and phases II and III (γ_2) was obtained mathematically as follows. First, a smoothed line was fitted to the relationship of Ψ_{pd} and Ψ_{md} that best described the data pattern. Subsequently, slope values (m) of the smoothed line were determined by $d\Psi_{md}/d\Psi_{pd}$ for d = 0.01 MPa, and maximum m in phase I ($=a$) and phase III ($=c$) and minimum m in phase II ($=b$) were identified. Parameters a, b, and c were used to determine γ_1 [$= (b - a)/2 + a$] and γ_2 [$= (c - b)/2 + b$].

Based on the information of γ_1 and γ_2, all parameters for the PLR model were fitted using a least-squares solver implemented in Python (pwfl package version 1.1.6; Jekel and Venter, 2019). This allowed for fitting a continuous piecewise linear function to corresponding data of Ψ_{pd} and Ψ_{md} for a specified number of three line segments. Our method used a limited memory Broyden-Fletcher-Goldfarb-Shanno algorithm for bound constrained optimization to obtain a statistical solution of boundary values Θ_1 and Θ_2 from the initial estimates of γ_1 and γ_2. SE and P values corresponding to output parameters of the PLR model were the result of using this optimization procedure to find boundaries Θ_1 and Θ_2 that best satisfied the specified number of linear segments; SE values were obtained following the derivation of Coppe et al. (2011) for linear regression problems.

Plant Materials

The WP curve method was tested initially for data collected during a drought screening trial on potted walnut trees (lathhouse trial). Subsequently, the method was further evaluated by reanalyzing data that were collected during drought screening trials of potted grapevines (greenhouse trial) and potted almond trees (open field trial) at the University of California, Davis. Therefore, growing conditions and experimental procedures for data collection for the three woody species were not identical and are best summarized as follows based on the information available.

Walnut Experiments

Experiments were performed in 2019 on n = 71 walnut trees ('Cisco'). Trees (stem diameter and height of around 2.5 cm and 1 m, respectively) were obtained from Sierra Gold Nursery and transplanted into 15-L plastic pots on February 17, 2019. Pots were filled with a similar amount of soil mix (~50% washed sand and 50% sphagnum peat moss) by leaving a gap of around 2 cm to the upper edge of the pot. A slow-release fertilizer (Osmocote Smart-Release Plus) was added to the topsoil layer. Growth was maintained under ambient atmospheric conditions (day/night length was on average 14/10 h, and temperature was ~13°C/32°C) in a lathhouse at the University of California, Davis. Trees were irrigated by supplying water to the top of the soil every 2 d and maintained well-watered for 3 months after transplanting to ensure sufficient time for tree establishment. All physiological measurements were performed on mature leaves of current-year shoots. A temperature and relative humidity sensor (HMP50; Vaisala) was installed at the plot site to monitor VPD (Supplemental Fig. S5). To investigate possible effects of the type of drought experiment, trees were subjected to a slow drydown (i.e. weeks, adjustment of irrigation) or a fast drydown (i.e. days, no supplemental irrigation). The slow drydown experiment was performed on n = 65 trees. Irrigation was adjusted based on estimates of bulk soil moisture (SM; = $\text{weight}_{H2O}/\text{weight}_{H2O\text{-pot-capacity}} \times 100\%$) as calculated from pot weights (for details, see Knipfer et al., 2020). A subset of n = 27 plants was located on mini-weighing lysimeters to continuously monitor pot weight and SM (see Supplemental Fig. S6 for representative data of two individuals); to account for temporal effects, trees were either maintained well-watered or subjected to a drydown. At 103 d after transplanting, measurements were performed on n = 27 trees with SM of individuals ranging from 40% to 90% (w/w; VPD ranged from 2.1 to 2.9 kPa between 11 AM and 1 PM). At 150 d after transplanting, measurements were carried out on n = 36 trees with SM ranging from 58% to 87% (w/w; VPD ranged from 1.9 to 2.5 kPa). At 162 d after transplanting, measurements were performed on n = 30 trees with SM ranging from 44% to 75% (w/w; VPD ranged from 1.7 to 2.2 kPa). The fast drydown experiment was performed on n = 6 trees that were maintained well-watered until the start of the drydown. Supplemental irrigation was stopped at 210 d after transplanting. Trees were analyzed at 210 d (SM ranging from 73% to 100% [w/w]), 213 d (69% to 96% [w/w]), 216 d (54% to 86% [w/w]), 218 d (49% to 77% [w/w]), and 220 (47% to 72% [w/w]) after transplanting.

Ψ

A pressure chamber (PMS Instrument; model 1505D) was used to measure plant Ψ following leaf covering and equilibration (Fig. 10). Measurements were performed on a leaflet of a mature leaf that was covered with aluminum foil and equilibrated for more than 1 h using a sealed plastic bag. Following excision of the leaflet at the petiolule, the plastic bag was removed and leaflets still covered with foil (i.e. to exclude effects of transpiration; Turner and Long 1980) were inserted into the pressure chamber. The pressure in the chamber was raised slowly at a constant rate (about 0.01 MPa s^{-1}), and pressure was recorded when a water meniscus started to form on the cut petiolule (midvein of leaflet) surface. For the same plant, Ψ_{pd} was measured prior to sunrise between 4 and 6 AM and Ψ_{md} was measured between 11 AM and 1 PM Pacific Daylight Time. Watering was always completed the day before measurement of plant Ψ to allow for soil water distribution.

Leaf Gas Exchange

g_s and A were measured between 11 AM and 1 PM using a LICOR-6800 gas-exchange system (fan speed at 10,000 rpm, leaf temperature at 24.5°C, CO_2 sample at 400 μL L^{-1}, and 1,500 μmol m^{-2} s^{-1} light intensity). One nonshaded leaflet of a mature leaf was measured on each sapling that was in proximity to the leaflet used for measurements of plant Ψ (as described above). Since the leaf area inserted in the cuvette of the gas-exchange system during measurement occupies many stomata and the response of individual stomates within this area can be more or less coordinated, the point of stomatal closure was defined as the point where g_s was reduced by around 90%.

P *and* π

From the same leaf used for plant Ψ and leaf gas exchange, a leaflet was excised with scissors. Immediately after the leaf lamina was separated from the midvein using a razor blade (i.e. to minimize the contribution of apoplastic xylem sap), the leaf lamina (a 2-cm-long portion located halfway along the leaflet) was placed in a 2-mL Eppendorf tube containing a mesh filter and stored on ice. Great care was taken to ensure that the procedure, from initial leaflet excision to storage of the Eppendorf tube on ice, was completed within 30 s to minimize drying artifacts. All samples were kept on ice, transported to the laboratory within 1 h following sampling, and stored at −80°C until further analysis. For analysis of leaf sap π, samples were thawed at room temperature for 15 to 20 min, centrifuged at 8,000 rpm for 15 min to extract leaf sap, and the osmolality of leaf sap was measured using a vapor pressure osmometer (VAPRO 5600; Wescor; (Barrios-Masias et al., 2019; Knipfer et al., 2020). Measured values of sap osmolality (in mOsmol kg^{-1}) were converted to units of π (0.1 MPa = 40.75 mOsmol kg^{-1}). P was estimated by $\Psi - \pi$ according to Jones and Truner (1978). Ψ_{TLP} was determined from pressure-volume curves measured on a leaflet. Prior to measurements, one mature leaf per plant was excised, the cut end of the petiole was submerged in water, and the leaf was covered with a plastic bag and transported to the lab within 30 min. Subsequently, the leaf was allowed to rehydrate in the darkness for 24 h. A leaflet was excised from the compound leaf, and Ψ_{TLP} was measured using the benchtop drydown method as described by Sack and Pasquet-Kok (2010). Leaflet fresh weight was measured with a digital balance before and after each Ψ step measurement (PMS Instrument; model 1505D). Measurements were repeated until five measurements after the Ψ_{TLP}.

Grapevine Experiments

Experiments were performed in 2019 on 48 grafted vines (cv Chardonnay on rootstocks 5C, 420A, Riparia Gloire, 101-14, Ramsey, 140Ru, 1103P, and 110R).

Vines were planted in 6-L pots. Pots were filled with similar amounts of soil mix (approximately 75% coconut coir and 25% perlite) by leaving a gap of around 2 cm to the upper edge of the pot. Growth was maintained in a greenhouse on the University of California, Davis, campus. Vines were allowed to establish for 3 months prior to data collection. During the establishment period, the vines were pruned to a single shoot, which was staked and tied after reaching approximately 0.5 m in length. The pots were weighed and irrigated by supplying water to the top of the soil three times per week to a target weight (pot weight at saturation + half of pot evapotranspiration; evapotranspiration was the difference in pot weights). On September 9, half of the vines were randomly assigned to each of two watering treatments. The well-watered vines continued to receive the same watering regime as during the establishment period, while the water-stressed vines were watered to 40% of the saturated pot weight plus half of pot evapotranspiration. Water was withheld from water-stressed vines until the pots reached the target weight. Three vines per rootstock × treatment combination (n = 48) were assessed for gas exchange and Ψ_{pd} and Ψ_{md} on November 4 and 12. On December 9, supplemental watering was stopped for one vine per rootstock from the water-stressed treatment to allow for severe drought conditions.

Ψ

A mature leaf was covered with a plastic bag just prior to excision from the stem using a razor blade (midday between 1 and 3 PM and predawn between 4 and 6 AM; Fig. 10). Subsequently, the bagged leaf was inserted in a sealed plastic bag and stored in a cooler (at 4°C). Leaves were transported to the laboratory, and Ψ_{pd} and Ψ_{md} was measured within 24 h following leaf excision using a pressure chamber following the procedure as described for the walnut experiment. Watering was always completed the day before measurement of plant Ψ to allow for soil water distribution.

Leaf Gas Exchange

Measurements were performed for one mature, fully expanded leaf per vine that was in proximity to the leaf used for Ψ measurements. The sampled leaves were selected from exterior, sunlit canopy positions. The gas-exchange measurements were conducted at the same time as plant Ψ measurements using a LICOR-6800 gas-exchange system at a constant fan speed (10,000 rpm), sample chamber VPD (1.5 kPa), CO_2 concentration (400 μL L^{-1}), and light intensity (1,000 μmol m^{-2} s^{-1}). Leaf temperature ranged from 26.9°C to 27.5°C.

Almond Experiments

Experiments were performed in 2014 on n = 16 potted 4-year-old almond trees ('Nonpareil' grafted on rootstock Nemaguard). Pots (56 L) were filled with similar amounts of soil mix (approximately 60% plaster sand and 40% peat moss). Slow-release fertilizer spikes (Miracle-Gro Fruit Fertilizer) were inserted in each pot. Potted trees were maintained in an open field at the Orchard Park Greenhouse Complex at the University of California, Davis, campus. Throughout the experimental period, the daily maximum temperature ranged from 19.4°C to 50.6°C. Over the experimental period, trees were watered by supplying water to the top of the soil either once every other day (n = 8 trees) or twice daily (n = 8 trees).

Ψ

Three mature leaves near the trunk were selected from each tree to perform Ψ_{pd} (5 AM to 6 AM) and Ψ_{md} (12 PM to 1 PM) measurements with a pressure chamber (PMS Instrument; model 1000). Leaves were covered with an aluminum foil bag and equilibrated for 15 min (predawn) and 45 min (midday; Fig. 10). Following excision, bagged leaves were sealed and transported in a cooler (at 4°C) to the laboratory, and plant Ψ measurements with the pressure chamber (as described for the walnut experiment) were performed within 1 h after leaf excision. Watering was always completed the day before measurement of plant Ψ to allow for soil water distribution.

Data Analysis

Graphs were generated using SigmaPlot (version 8.0; Systat Software). Smoothed lines that best described the pattern of data points were generated using the PROC TRANSREG procedure in SAS (version 9.2; SAS Institute). A statistical comparison of model output parameters was performed using a Z test (Supplemental Table S2).

Supplemental Data

The following supplemental materials are available.

Supplemental Figure S1. Recordings of pot weight and bulk soil moisture for walnut trees.

Supplemental Figure S2. Representative images of the canopy of walnut trees.

Supplemental Figure S3. Ψ curve collected for walnut genotypes RX1 and VX211.

Supplemental Figure S4. Relationship between Ψ and canopy conductance of walnut trees.

Supplemental Figure S5. Recordings of VPD for walnut trees.

Supplemental Figure S6. Relationship of Ψ_{pd} and bulk soil moisture of walnut trees.

Supplemental Table S1. Ψ_{TLP} determined from pressure-volume curves for walnut trees.

Supplemental Table S2. Z test used for statistical comparison of output parameters shown in Table 1.

ACKNOWLEDGMENTS

We thank the California Walnut Board and Sierra Gold Nursery for providing the plant material, Dr. Andrew Walker (University of California, Davis) as a collaborator on the American Vineyard Foundation grant that supported grapevine research, and Dr. Kenneth Shackel (University of California, Davis) for helpful comments on an earlier version of this article. We would like to thank Dr. Steffen Docken (University of New South Wales) for his advise in designing the PLR model. We also thank the anonymous reviewers for their helpful comments and suggestions.

Received April 24, 2020; accepted July 21, 2020; published August 6, 2020.

LITERATURE CITED

Alsina MM, De Herralde F, Aranda X, Save R, Biel C (2007) Water relations and vulnerability to embolism are not related: Experiments with eight grapevine cultivars. Vitis **46:** 1–6

Aroca R, Porcel R, Ruiz-Lozano JM (2012) Regulation of root water uptake under abiotic stress conditions. J Exp Bot **63:** 43–57

Barrios-Masias FH, Knipfer T, Walker MA, McElrone AJ (2019) Differences in hydraulic traits of grapevine rootstocks are not conferred to a common *Vitis vinifera* scion. Funct Plant Biol **46:** 228–235

Barrios-Masias FH, Knipfer T, McElrone AJ (2015) Differential responses of grapevine rootstocks to water stress are associated with adjustments in fine root hydraulic physiology and suberization. J Exp Bot **66:** 6069–6078

Blum A (2017) Osmotic adjustment is a prime drought stress adaptive engine in support of plant production. Plant Cell Environ **40:** 4–10

Blum A, Ebercon A (1981) Cell membrane stability as a measure of drought and heat tolerance in wheat. Crop Sci **21:** 43–47

Brodersen CR, McElrone AJ, Choat B, Lee EF, Shackel KA, Matthews MA (2013) In vivo visualizations of drought-induced embolism spread in *Vitis vinifera*. Plant Physiol **161:** 1820–1829

Brodribb TJ, Holbrook NM (2003) Stomatal closure during leaf dehydration, correlation with other leaf physiological traits. Plant Physiol **132:** 2166–2173

Brodribb TJ, McAdam SAM (2011) Passive origins of stomatal control in vascular plants. Science **331:** 582–585

Brodribb TJ, McAdam SAM (2017) Evolution of the stomatal regulation of plant water content. Plant Physiol **174:** 639–649

Carminati A, Javaux M (2020) Soil rather than xylem vulnerability controls stomatal response to drought. Trends Plant Sci **25:** 868–880

Choat B, Brodribb TJ, Brodersen CR, Duursma RA, López R, Medlyn BE (2018) Triggers of tree mortality under drought. Nature **558:** 531–539

Choat B, Drayton WM, Brodersen C, Matthews MA, Shackel KA, Wada H, McElrone AJ (2010) Measurement of vulnerability to water stress-induced

cavitation in grapevine: A comparison of four techniques applied to a long-vesseled species. Plant Cell Environ **33:** 1502–1512

Cochard H, Forestier S, Améglio T (2001) A new validation of the Scholander pressure chamber technique based on stem diameter variations. J Exp Bot **52:** 1361–1365

Coppe A, Haftka RT, Kim NH (2011) Uncertainty identification of damage growth parameters using nonlinear regression. AIAA J **49:** 2818–2821

Couchoud M, Der C, Girodet S, Vernoud V, Prudent M, Leborgne-Castel N (2019) Drought stress stimulates endocytosis and modifies membrane lipid order of rhizodermal cells of *Medicago truncatula* in a genotype-dependent manner. BMC Plant Biol **19:** 221

Cuneo IF, Knipfer T, Brodersen CR, McElrone AJ (2016) Mechanical failure of fine root cortical cells initiates plant hydraulic decline during drought. Plant Physiol **172:** 1669–1678

Ding Y, Zhang Y, Zheng QS, Tyree MT (2014) Pressure-volume curves: Revisiting the impact of negative turgor during cell collapse by literature review and simulations of cell micromechanics. New Phytol **203:** 378–387

Dixon HH, Joly J (1895) On the ascent of sap. Proc R Soc Lond **57:** 3–5

Donovan L, Linton M, Richards J (2001) Predawn plant water potential does not necessarily equilibrate with soil water potential under well-watered conditions. Oecologia **129:** 328–335

Farquhar GD, Sharkey TD (1982) Stomatal conductance and photosynthesis. Annu Rev Plant Biol **61:** 561–591

Franks PJ (2013) Passive and active stomatal control: Either or both? New Phytol **198:** 325–327

Fricke W, Peters WS (2002) The biophysics of leaf growth in salt-stressed barley: A study at the cell level. Plant Physiol **129:** 374–388

Gilbert ME, Medina V (2016) Drought adaptation mechanisms should guide experimental design. Trends Plant Sci **21:** 639–647

Gollan T, Passioura JB, Munns R (1986) Soil water status affects the stomatal conductance of fully turgid wheat and sunflower leaves. Aust J Plant Physiol **13:** 459–464

Gollan T, Turner NC, Schulze ED (1985) The responses of stomata and leaf gas exchange to vapour pressure deficits and soil water content. III. In the sclerophyllous woody species Nerium oleander. Oecologia **65:** 356–362

Jekel C, Venter G (2019) A python library for fitting 1D continuous piecewise linear functions. https://github.com/cjekel/piecewise_linear_fit_py (July 14, 2020)

Jones HG (2007) Monitoring plant and soil water status: Established and novel methods revisited and their relevance to studies of drought tolerance. J Exp Bot **58:** 119–130

Jones MM, Truner NC (1978) Osmotic adjustment in leaves of sorghum in response to water deficits. Plant Physiol **61:** 122–126

Klepper B (1968) Diurnal pattern of water potential in woody plants. Plant Physiol **43:** 1931–1934

Knipfer T, Barrios-Masias FH, Cuneo IF, Bouda M, Albuquerque CP, Brodersen CR, Kluepfel DA, McElrone AJ (2018) Variations in xylem embolism susceptibility under drought between intact saplings of three walnut species. Tree Physiol **38:** 1180–1192

Knipfer T, Brodersen CR, Zedan A, Kluepfel DA, McElrone AJ (2015) Patterns of drought-induced embolism formation and spread in living walnut saplings visualized using x-ray microtomography. Tree Physiol **35:** 744–755

Knipfer T, Fei J, Gambetta GA, Shackel KA, Matthews MA (2014) A revised and unified pressure-clamp/relaxation theory for studying plant cell water relations with pressure probes: In-situ determination of cell volume for calculation of volumetric elastic modulus and hydraulic conductivity. J Theor Biol **359:** 80–91

Knipfer T, Reyes C, Earles JM, Berry ZC, Johnson DM, Brodersen CR, McElrone AJ (2019) Spatiotemporal coupling of vessel cavitation and discharge of stored xylem water in a tree sapling. Plant Physiol **179:** 1658–1668

Knipfer T, Reyes C, Momayyezzi M, Kluepfel D, McElrone AJ (2020) A comparative study on physiological responses of commercially available walnut genotypes (RX1, Vlach and VX211) to drought stress. Trees (Berl) **34:** 665–678

Marsal J, Girona J, Mata M (1997) Leaf water relation parameters in almonds compared to hazelnut trees during a deficit irrigation period. J Am Soc Hortic Sci **122:** 582–587

Martínez-Vilalta J, Poyatos R, Aguadé D, Retana J, Mencuccini M (2014) A new look at water transport regulation in plants. New Phytol **204:** 105–115

Martínez-Vilalta J, Garcia-Forner N (2017) Water potential regulation, stomatal behaviour and hydraulic transport under drought: Deconstructing the iso/anisohydric concept. Plant Cell Environ **40:** 962–976

Martin-StPaul N, Delzon S, Cochard H (2017) Plant resistance to drought depends on timely stomatal closure. Ecol Lett **20:** 1437–1447

McAdam SAM, Brodribb TJ (2018) Mesophyll cells are the main site of abscisic acid biosynthesis in water-stressed leaves. Plant Physiol **177:** 911–917

McDowell N, Allen CD, Anderson-Teixeira K, Brando P, Brienen R, Chambers J, Christoffersen B, Davies S, Doughty C, Duque A, et al (2018) Drivers and mechanisms of tree mortality in moist tropical forests. New Phytol **219:** 851–869

Meinzer FC, Woodruff DR, Marias DE, Smith DD, McCulloh KA, Howard AR, Magedman AL (2016) Mapping 'hydroscapes' along the iso- to anisohydric continuum of stomatal regulation of plant water status. Ecol Lett **19:** 1343–1352

Meyer CJ, Seago JL Jr., Peterson CA (2009) Environmental effects on the maturation of the endodermis and multiseriate exodermis of *Iris germanica* roots. Ann Bot **103:** 687–702

Premachandra GS, Shimada T (1987) The measurement of cell membrane stability using polyethylene glycol as a drought tolerance test in wheat. Jpn J Crop Sci **56:** 92–98

Ratzmann G, Meinzer FC, Tietjen B (2019) Iso/anisohydry: Still a useful concept. Trends Plant Sci **24:** 191–194

Rhizopoulou S (1997) Is negative turgor fallacious? Physiol Plant **99:** 505–510

Rodriguez-Dominguez CM, Brodribb TJ (2020) Declining root water transport drives stomatal closure in olive under moderate water stress. New Phytol **225:** 126–134

Sack L, Pasquet-Kok J (2010) Leaf pressure-volume curve parameters. PrometheusWiki. http://prometheuswiki.org/tiki-index.php?page=Leaf+pressure-volume+curve+parameters (August 27, 2020)

Scholander PF, Bradstreet ED, Hemmingsen EA, Hammel HT (1965) Sap pressure in vascular plants: Negative hydrostatic pressure can be measured in plants. Science **148:** 339–346

Scoffoni C, Albuquerque C, Cochard H, Buckley TN, Fletcher LR, Caringella MA, Bartlett M, Brodersen CR, Jansen S, McElrone AJ, et al (2018) The causes of leaf hydraulic vulnerability and its influence on gas exchange in *Arabidopsis thaliana*. Plant Physiol **178:** 1584–1601

Shackel KA, Ahmadi H, Biasi W, Buchner R, Goldhamer D, Gurusinghe S, Hasey J, Kester D, Krueger B, Lampinen B, et al (1997) Plant water status as an index of irrigation need in deciduous fruit trees. HortTechnology **7:** 23–28

Staverman AJ (1951) The theory of measurement of osmotic pressure. Recl Trav Chim Pays Bas **70:** 344–352

Tardieu F, Simonneau T (1998) Variability among species of stomatal control under fluctuating soil water status and evaporative demand: Modelling isohydric and anisohydric behaviours. J Exp Bot **49:** 419–432

Tombesi S, Nardini A, Frioni T, Soccolini M, Zadra C, Farinelli D, Poni S, Palliotti A (2015) Stomatal closure is induced by hydraulic signals and maintained by ABA in drought-stressed grapevine. Sci Rep **5:** 12449

Tomos AD, Leigh RA (1999) The pressure probe: A versatile tool in plant cell physiology. Annu Rev Plant Physiol Plant Mol Biol **50:** 447–472

Torrecillas A, Alarcon JJ, Domingo R, Planes J, Sachez-Blanco MJ (1996) Strategies for drought resistance in leaves of two almond cultivars. Plant Sci **118:** 135–143

Turner NC (1981) Techniques and experimental approaches for the measurement of plant water status. Plant Soil **58:** 339–366

Turner NC (1990) Plant water relations and irrigation management. Agric Water Manage **17:** 59–73

Turner NC (2019) Imposing and maintaining soil water deficits in drought studies in pots. Plant Soil **439:** 45–55

Turner NC, Long MJ (1980) Errors arising from rapid water loss in the measurement of leaf water potential by the pressure chamber technique. Aust J Plant Physiol **7:** 527–537

Tyree MT (1976) Negative turgor pressure in plant cells: Fact or fallacy? Can J Bot **54:** 2738–2746

Tyree MT, Hammel HT (1972) The measurement of the turgor pressure and the water relations of plants by the pressure-bomb technique. J Exp Bot **23:** 267–282

Wardlaw IF (2005) Consideration of apoplastic water in plant organs: A reminder. Funct Plant Biol **32:** 561–569

Williams LE, Araujo FL (2002) Correlations among predawn leaf, midday leaf, and midday stem water potential and their correlations with other measures of soil and plant water status in *Vitis vinifera*. J Am Soc Hortic Sci **127:** 448–454

Zhang J, Schurr U, Davies WJ (1987) Control of stomatal closure behavior by abscisic acid which apparently originates in the roots. J Exp Bot **38:** 1174–1181

Zhu J, Brown KM, Lynch JP (2010) Root cortical aerenchyma improves the drought tolerance of maize (*Zea mays* L.). Plant Cell Environ **33:** 740–749